Proc. Natl. Acad. Sci. USA
Vol. 95, pp. 3966–3971, March 1998
Neurobiology

Neuronal polarity: Essential role of protein–lipid complexes in axonal sorting

MARIA DOLORES LEDESMA, KAI SIMONS, AND CARLOS G. DOTTI*

Cell Biology Program, European Molecular Biology Laboratory, 69112 Heidelberg, Germany

Contributed by Kai Simons, February 3, 1998

ABSTRACT **The viral glycoprotein hemagglutinin (HA) and the endogenous glycosylphosphatidylinositol-anchored protein Thy-1 are efficiently targeted to the axonal surface of fully polarized hippocampal neurons in culture. Here we have shown that in these cells HA and Thy-1 interact with sphingolipid–cholesterol rafts and are included in detergent-insoluble glycolipid-enriched complexes. Axonal HA and Thy-1, but not two dendritic membrane proteins, resisted extraction to detergents at 4°C. Both HA and Thy-1 became detergent-soluble in neurons with reduced levels of cholesterol or sphingolipids. Missorting of the axonal Thy-1 but not of a dendritic membrane protein occurred in sphingolipid-deprived cells. These results indicate that neurons sort a subset of axolemmal proteins by a mechanism that requires the formation of protein–lipid rafts. The involvement of rafts in axonal membrane sorting may explain the neurological deficits observed in patients with certain types of Niemann–Pick disease.**

To understand the mechanisms involved in the segregation of axonal and dendritic membrane proteins, we analyzed in the past the intracellular trafficking of overexpressed viral and endogenous membrane proteins (1, 2). We observed that infection of mature hippocampal neurons with fowl plague virus (FPV) resulted in axonal delivery of the hemagglutinin (HA) glycoprotein. Given that HA is preferentially delivered to the apical surface of the epithelial MDCK cells we postulated that the axonal sorting machinery may be similar to that responsible for the generation of the apical surface of epithelial cells. This hypothesis was strengthened by the finding that a glycosylphosphatidylinositol (GPI)-anchored protein, apical in MDCK cells, is axonal in neurons (3). Subsequent work has demonstrated that many apical and basolateral proteins are axonal and somatodentritic, respectively (4, 5). Although several exceptions exist, this is not surprising because proteins that are basolateral in certain epithelial cells are apical in others (6, 7). Therefore, the relationships between apical and axonal sorting can only be revealed by dissection of the underlying molecular machinery in both cell types. In epithelial cells certain apical proteins, including influenza HA and GPI-anchored proteins, form detergent-insoluble sphingolipid–cholesterol rafts that are thought to function as platforms for apical delivery (8). In this paper we have analyzed whether this mechanism is involved in axonal sorting in fully polarized hippocampal neurons.

The lipid raft concept emerged from the early observations that the apical and basolateral surfaces of epithelial cells have different lipid compositions (9, 10). The external leaflet of the apical surface is enriched in glycosphingolipids (GSL) whereas on the basolateral side phosphatidylcholine dominates. The enrichment of glycosphingolipids is postulated to occur in the luminal face of the trans-Golgi network (TGN) membrane (10). There, GSL, sphingomyelin, and certain proteins cluster together forming rafts (10, 11). Later, it was demonstrated that raft-associated proteins do not become solubilized upon treatment with detergents such as 3-[(3-cholamidopropyl)dimethylammonio]-1-propanesulfonate (CHAPS), Triton X-100, and Triton X-114 at 4°C (12–14) but form detergent-insoluble glycosphingolipid-sphingomyelin-cholesterol complexes (DIGs). Although the precise mechanism by which sphingolipid–cholesterol rafts operate is not clear, support for their role in apical sorting came from the finding that two different kinds of apical proteins, GPI-anchored proteins and HA, are part of DIGs (12, 14, 15) and that basolateral proteins are not (14). Reconstitution and other experiments later demonstrated that it is the interaction with sphingolipids and cholesterol that confers detergent insolubility (16–18).

Given that HA and Thy-1 are sorted to the axon of fully polarized neurons (1, 3), the rationale behind our interest in analyzing the role of rafts in neuronal sorting becomes clear. If the hypothesis is correct at the molecular level one would predict to find these axonal proteins in DIGs in polarized neurons and their sorting dependent on DIG integrity. Here we show that in mature hippocampal neurons HA and Thy-1 are axonal and are present in DIGs rafts, and that reduction of raft lipid levels leads to decreased DIG formation and membrane missorting.

MATERIALS AND METHODS

Cell Culture, Virus Infections, and Immunofluorescence Microscopy. Cultures of hippocampal cells were prepared from the brains of 18-day-old rat embryos as described in Goslin and Banker (19). For our experiments, cells were kept in culture for 8–15 days (stage 5 neurons). Viral stocks were prepared as described in Matlin *et al.* (20) and Fuller *et al.* (21). Cultured hippocampal cells were infected with 1–10 pfu/cell in N_2 medium of either FPV or Semliki Forest virus (SFV) (1–2). After 1–2 hr infection at 37°C the virus-containing medium was replaced by fresh N_2 and the cells were further incubated for different times (3–7 hr). To label intracellular [HA, glutamate receptor subunit 1 (GluR1), microtubule-associated protein 2 (MAP2)] and surface (Thy-1) proteins, cells were processed for immunofluorescence as described (1, 2). The following primary antibodies were used: rabbit anti-HA (20), mouse anti-Thy 1.1 (clone number MRC OX-7 from Serotec), polyclonal antibody 514 anti-MAP2 (a gift from C. Sanchez, Centro de Biologia Molecular, Madrid), mAb anti-MAP2 (Amersham), and polyclonal antibody anti-GluR1 (Upstate

Abbreviations: HA, hemagglutinin; FPV, fowl plague virus; GPI, glycosyl-phosphatidyl inositol; DIG, detergent-insoluble glycosphingolipid-sphingomyelin-cholesterol complexes; MAP2, microtubule-associated protein 2; SFV, Semliki Forest virus; TGN, trans-Golgi network; GSL, glycosphingolipid; FB1, fumonisin 1B; GluR1, AMPA glutamate receptor subunit 1; CHAPS, 3-[(3-cholamidopropyl)dimethylammonio]-1-propanesulfonate.

*To whom reprint requests should be addressed. e-mail: dotti@embl-heidelberg.de.

The publication costs of this article were defrayed in part by page charge payment. This article must therefore be hereby marked "*advertisement*" in accordance with 18 U.S.C. §1734 solely to indicate this fact.

Biotechnology). Incubations were performed for 1 hr at room temperature. After extensive washing with PBS, cells were incubated with species-specific secondary antibodies.

Quantification of HA and Thy-1 Distribution. Stage 5 neurons were processed for immunofluorescence by using antibodies against the dendritic marker MAP2 and against Thy-1 or, in the case of FPV-infected neurons, against HA. Phase-contrast, MAP2, and HA/Thy-1 images were captured with a charge-coupled device camera (Cohu 4910, Cohu, San Diego), connected to a Macintosh computer (Power Macintosh 7300/166) equipped with an image recorder (LG3, Scion, Frederick, MD). Unprocessed images were stored by using NIH IMAGE, and without further modification, images with HA- and Thy-1-labeled cells were density sliced, axonal and dendritic segments (identified by comparison of these images with the corresponding MAP2-positive, MAP2-negative, and phase-contrast images) were randomly chosen and delineated, the areas were binarized, and the signal within the area was quantitated (total surface/pixel intensity). Axonal and dendritic areas were normalized to the same size, and the average of labeling intensity in dendrites and axons was calculated.

Detergent Extractions. HA insolubility during transit along the biosynthetic pathway was analyzed as follows. Neurons were infected with FPV for 1 hr, and expression of HA was allowed for 3 more hours and then metabolically labeled in methionine-free N_2 medium containing 200 μCi/ml of [^{35}S]methionine for 30 min. After chase periods of 0, 90, and 180 min in fresh N_2 medium at 37°C neurons were washed in cold PBS, scraped, and extracted for 1 hr in 20 mM CHAPS/150 mM NaCl/50 mM Tris, pH 7.4/2 mM EDTA/2 mM DTT and a mixture of protease inhibitors containing 20 μg/ml aprotinin, chymostatin, pepstatin, and leupeptin (CLAP). Then the samples were centrifuged for 15 min at 15,000 $\times$ *g* and 4°C. Supernatants and pellets were collected and analyzed by 10–20% SDS/PAGE. Dried gels were visualized with a PhosphorImager (Molecular Dynamics).

For surface biotinylation experiments cells were infected for 6 hr with FPV and metabolically pulse-labeled for 30 min at 37°C with 200 μCi/ml [^{35}S]methionine in methionine-free N_2 medium. Then cells were chased for 2.5 hr in fresh N_2 medium to allow the labeled protein to reach the cell surface. After the chase, cells were washed with Ca/Mg-PBS and incubated on ice with freshly made membrane impermeant S-NHS-LC-Biotin (Pierce) for 30 min and processed as described (22).

For the immunofluorescence analysis of Thy-1 distribution after detergent extraction, neurons on coverslips were washed in PBS, incubated 1 min in cold microtubule stabilizing buffer (MSB; 2 mM $MgCl_2$/10 mM EGTA/60 mM Pipes, pH 7.0) and extracted for 8 min on ice with 1% Triton X-100 diluted in MSB. After a final washing with cold MSB, the cells were fixed with 4% paraformaldehyde and processed for immunofluorescence by using anti-Thy-1 antibody.

For the biochemical analysis of Thy-1 insolubility in Triton X-114, a protocol adapted from Lisanti *et al.* (23) was used. Cells were extracted for 1 hr at 4°C in TBS (10 mM Tris, pH 7.4/150 mM NaCl/1 mM EDTA and CLAP) containing 1% Triton X-114. Insoluble material was pelleted by a 15-min centrifugation at 15,000 $\times$ *g* at 4°C.

Flotation experiments in sucrose gradients of detergent-extracted HA, E2, and GluR1 were performed as in Brown and Rose (13). The different fractions were analyzed by Western blotting using antibodies against HA and GluR1 and a mouse monoclonal anti-E2 glycoprotein (9AB4) (24).

Fumonisin Treatment. Fumonisin B1 (FB1) (Sigma) was added from a 1-mM stock solution in 20 mM Hepes, pH 7.4, to neurons 24 hr after being plated on coverslips. FB1 was subsequently added every 48 hr to final concentrations of 10 μM, 25 μM, or 40 μM depending on the experiment. After 8 days of treatment the cells were processed for detergent extraction and/or immunofluorescence by using anti-Thy-1, MAP2, and GluRc1 antibodies as described above.

Cholesterol Depletion. After 5 days in culture 4 μM lovastatin (kindly provided by Renate Luedecke, MSD Sharp & Dome, Haar, Germany) and 0.25 mM mevalonate (Sigma) were added or not to the neuronal medium. On day 9 the treated and untreated neurons were infected with FPV for 2 hr, then the viral medium was replaced by control N_2 or N_2 containing 4 μM lovastatin and 0.25 mM mevalonate. After 3 more hours, the neurons treated with lovastatin and mevalonate were further incubated with 5 mM methyl-β-cyclodextrin (CD) (Sigma) for 15 min at 37°C in labeling N_2 medium without methionine. Control neurons were incubated for the same time with labeling medium without CD. The medium was aspirated and labeling medium containing 200 μCi/ml [^{35}S]methionine was added for 12 min to all the samples. Control and treated samples were collected immediately after the pulse (0 min) or after 25- and 60-min chases in either normal N_2 medium for the controls or N_2 medium containing lovastatin and mevalonate for the CD-treated. The samples were extracted for 1 hr in 1% Triton X-100/150 mM NaCl/50 mM Tris, pH 7.4/2 mM EDTA/2 mM DTT/CLAP and centrifuged for 15 min at 15,000 $\times$ *g* and 4°C. Supernatants and pellets were collected and submitted to a 10–20% SDS/PAGE. Dried gels were finally analyzed by PhosphorImager. The bands corresponding to the mature form of HA were quantified by densitometry and expressed as a percentage of total HA (soluble and insoluble) in each chasing point.

RESULTS

Overexpressed HA Is Axonal and Present in DIGs in Fully Mature Neurons. In our first series of experiments we quantitatively analyzed the axonal delivery of HA (Fig. 1). Fully mature hippocampal neurons were infected with wild-type FPV and fixed 6 hr later, and the axonal and dendritic distribution of HA was determined by indirect immunofluorescence microscopy. The dendrites of the cells were labeled by using an antibody against MAP2, a cytoskeletal dendritic protein (25) (Fig. 1*A*). Twelve infected neurons expressing HA from two different experiments were chosen for quantification (an example is shown in Fig. 1*B*). Our quantitative method (see *Materials and Methods* and Fig. 1*C*) revealed preferential delivery of HA to the axon. We observed that of the total HA in processes, 78% is in axons and 22% is in dendrites. However, there is cell variation, and some cells show more than 90% of axonal HA (n = 6) whereas in others axonal HA ranges from 55% (n = 2) to 60–70% (n = 4) (Fig. 1*D*). These results confirm quantitatively our earlier report on the preferential axonal delivery of HA (1, 2).

We tested next whether in hippocampal neurons HA acquired resistance to detergent extraction during intracellular transport (Fig. 2*A*). Mature stage 5 neurons were infected, the newly synthesized HA was metabolically labeled, and the appearance of resistance to detergent extraction was determined at different times by exposing the cell lysate to CHAPS at 4°C. At time 0 most of the mature complex-glycosylated HA (higher molecular weight band) is soluble. At 90 and 180 min, however, the mature HA becomes increasingly resistant to detergent extraction, thus remaining in the insoluble pellet. The immature form of HA (the high-mannose form that has a lower molecular weight) remains in the endoplasmic reticulum (ER) and is present only in the soluble fractions.

To determine whether HA remained in detergent-resistant complexes after insertion into the plasma membrane, solubility was measured by surface biotinylation followed by extraction in CHAPS at 4°C (Fig. 2*B*). In fully polarized hippocampal cells most surface HA was present in the insoluble fraction (87%).

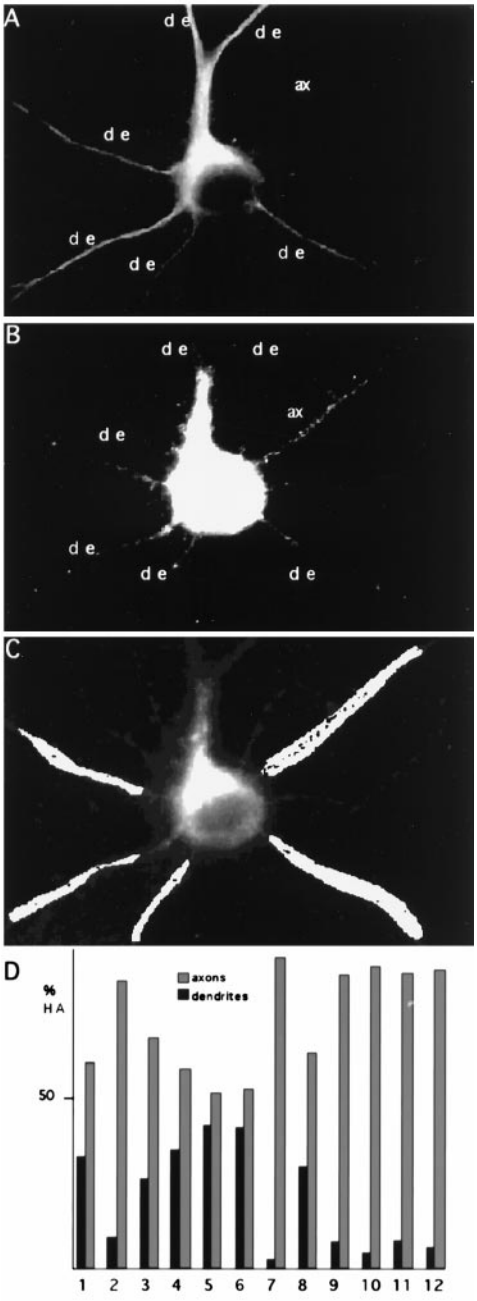

FIG. 1. Axonal distribution of HA in stage 5 neurons. (*A*) FPV-infected stage 5 neuron stained with an antibody against the dendritic marker MAP2; the axon (ax) appears devoid of labeling. (*B*) The same infected neuron was coimmunostained with an antibody against HA. The labeling is mainly present in the axon (ax), leaving the dendrites (de) almost unstained. This was quantified by binarizing the image in *B* and choosing at random similar areas in dendrites and axons as is shown in *C*. The number of pixels was analyzed and normalized to the same area size in each process. (*D*) Percentage of HA present in dendrites versus axons in 12 different neurons. The mean value for the distribution of HA is 78% in the axons and 22% in the dendrites.

Altogether these results show that in mature neurons HA acquires resistance to detergent extraction during transit through the Golgi apparatus and remains detergent-insoluble in the plasma membrane. This is identical to the biochemical behavior of HA in the kidney epithelial MDCK cells (18).

To analyze whether detergent resistance of HA is due to partitioning into DIGs or to association with cytoskeletal elements, mature hippocampal neurons were infected for 8 hr with FPV, and the cell membrane fraction was extracted in 1%

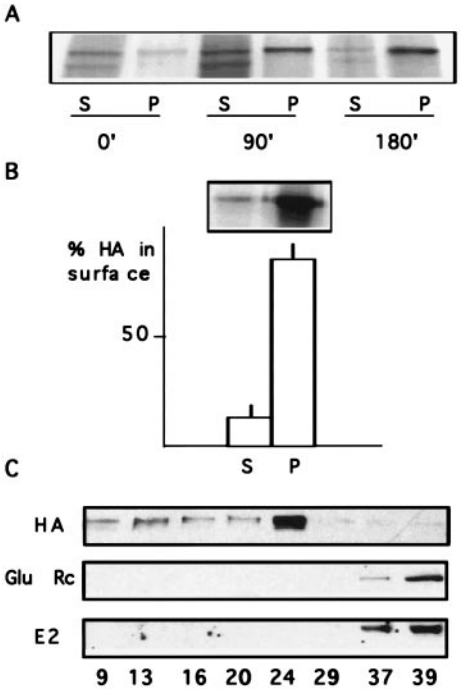

FIG. 2. HA insolubility in stage 5 neurons. (*A*) HA insolubility during the biosynthetic pathway. FPV-infected stage 5 neurons were metabolically labeled. After chases of 0, 90, or 180 min the cells were extracted with 20 mM CHAPS at 4°C and centrifuged. The amount of HA present in supernatants (S) and pellets (P) was determined by 10–20% SDS/PAGE and autoradiography. The mature form of HA becomes more and more insoluble with time. The lower-molecular-weight band present in the supernatants corresponds to the immature form of HA that remains in the ER. (*B*) HA insolubility on the surface. FPV-infected stage 5 neurons were biotinylated, and were CHAPS extracted. The resultant supernatants (S) and pellets (P) were analyzed by SDS/PAGE and autoradiography. Almost all surface HA is detergent-insoluble (87%). The graphic shows the data expressed as percent of the total surface HA and mean values ±SD from three different experiments. (*C*) Isolation of detergent-insoluble complexes. TX-100 extracts of stage 5 neurons infected with FPV (HA), noninfected (Glu Rc), or infected with SFV (E2) were prepared at 4°C and centrifuged to equilibrium in a sucrose gradient. Fractions of equal volume were collected and the amount of sucrose was determined with a refractometer (numbers at the bottom indicate percentage of sucrose). The fractions were analyzed by Western blot by using the following antibodies: anti-HA (HA), anti-AMPA glutamate receptor subunit 1 (Glu Rc), and anti-E2 (E2). HA from stage 5 cells is found in the lighter fractions (24–9% sucrose), revealing its interaction with lipids, whereas the dendritic proteins glutamate receptor and the viral E2 are found in the high density fractions (37 and 39% sucrose).

Triton X-100 at 4°C and subjected to flotation in a sucrose gradient (Fig. 2*C*). In mature neurons HA was present in the lighter fractions of the gradient (9–24% sucrose). This flotation experiment confirms that the detergent insolubility of HA at low temperatures is due to its binding to lipids and not to association with cytoskeletal proteins. Moreover, HA insolubility in stage 5 neurons resembles DIGs of nonneuronal cells (13, 14). To confirm that HA insolubility in the mature neurons is specific for this axonal protein and not due to viral protein overexpression we studied the detergent extractability of the SFV-E2 glycoprotein, which in mature neurons is delivered to the dendritic surface (2, 22). Stage 5 cells were infected with SFV for 8 hr, extracted in Triton X-100 at 4°C, and subjected to flotation in a sucrose gradient. In contrast to HA, the E2 glycoprotein remained in the heaviest fractions (37 and 39% sucrose) (Fig. 2*C*). Identical results were obtained for an endogenous membrane protein, the AMPA glutamate receptor subunit GluR1 (Fig. 2*C*), which, in stage 5 neurons, is exclusively dendritic (26).

The Endogenous Protein Thy-1 Is Axonal and Is Present in Detergent-Resistant Complexes in Fully Mature Neurons. We investigated next whether endogenous axonal membrane proteins are also included in DIGs. For this purpose we studied the distribution and behavior to detergent extraction of the GPI-anchored protein Thy-1. Quantitative analysis (Fig. 3 *A* and *B*) from three different experiments revealed that 80–95% of the surface Thy-1 is axonal (see also Figs. 4 and 5). To determine whether Thy-1 partitioned into detergent-resistant complexes, mature hippocampal neurons were solubilized in Triton X-114 at 4°C and the solubility of Thy-1 was determined biochemically. Western blot analysis of total Thy-1 revealed a significant proportion (33%) in the insoluble fraction (Fig. 3*C*). Resistance of Thy-1 to detergent extraction in the axons of the neurons was also demonstrated by immunofluorescence microscopy (Fig. 4 *A* and *B*).

Collectively, the results obtained for HA and Thy-1 show a correlation between axonal distribution and resistance to detergent extraction at 4°C.

Cholesterol and Sphingolipid Depletion Affects HA and Thy-1 Insolubility. To study the role of DIGs in axonal sorting we disturbed cholesterol and sphingolipid synthesis in fully mature neurons and analyzed the involvement of these lipids in the detergent insolubility of HA and Thy-1.

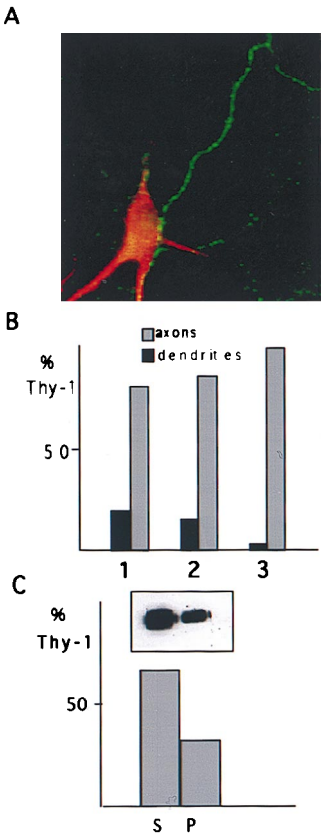

FIG. 3. Thy-1 distribution and insolubility in stage 5 neurons. (*A*) Double immunofluorescence of a stage 5 neuron using an antibody against the dendritic marker MAP2 (in red) and against Thy-1 (in green). The axonal distribution of surface Thy-1 is evident. (*B*) Quantitative analysis of Thy-1 distribution from three different experiments (1, 2, and 3). In each experiment an average number of eight dendrites (MAP2 positive) and eight axons were examined. The mean values of the Thy-1 labeling in axons versus dendrites are shown by histograms as a percentage of the total Thy-1 labeling observed in each experiment. Eighty to 95% of Thy-1 is axonal. (*C*) The soluble (S) and insoluble (P) fractions after extraction of cell lysates with 1% Triton X-114 at 4°C were analyzed by Western blot by using an antibody against Thy-1. A significant amount of the protein (33%) remains insoluble.

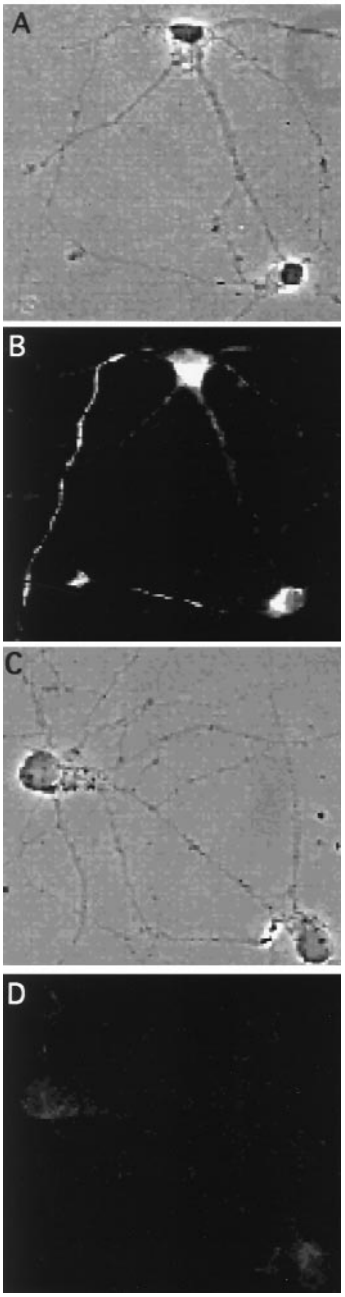

FIG. 4. Changes in Thy-1 insolubility in stage 5 neurons after inhibition of sphingolipid synthesis with fumonisin B1. Neurons were maintained in culture for 8 days in the absence (*A* and *B*) or presence (*C* and *D*) of 25 μM FB1. Then the cells were extracted in 1% Triton X-100, washed, fixed, and processed for immunofluorescence by using an antibody against Thy-1. (*A* and *B*) Phase contrast and Thy-1 staining, respectively, of control detergent-extracted neurons. The detergent is not able to solubilize the protein from the axon of the cells. (*C* and *D*) Phase contrast and Thy-1 staining, respectively, of FB1-treated, detergent-extracted neurons. In this case the detergent is able to remove the protein.

Cholesterol levels were decreased from neurons by using lovastatin (an inhibitor of HM-CoA reductase) (27) and methyl-β-cyclodextrin (which extracts cholesterol from cells) (28–30). Small amounts of mevalonate were also added to allow the synthesis of nonsterol products (31). Recent experiments revealed that this combination depletes about 70% of the cholesterol from hippocampal neurons (unpublished data) as well as from other cells (32) without affecting cell viability. In FPV-infected, metabolically labeled, cholesterol-depleted

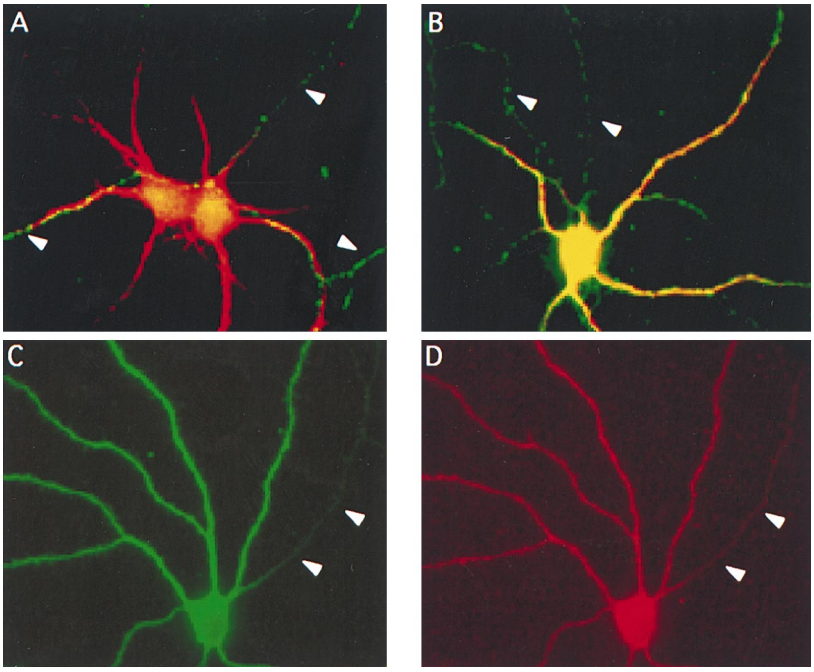

FIG. 5. Missorting of the axonal Thy-1 but not the dendritic GluR1 occurs in stage 5 neurons after incubation with fumonisin B1. Neurons were maintained in culture for 8 days in the absence (*A*) or presence (*B–D*) of 25 μM FB1. Then the cells were processed for double-immunofluorescence microscopy by using antibodies against MAP2 (*A–C*) and Thy-1 (*A* and *B*) or GluR1 (*D*). MAP2 is restricted to the dendrites and serves as a marker for these processes in control and treated cells. (*A* and *B*) Overlay of MAP2 (in red) and Thy-1 (in green) staining in control (*A*) and FB1-treated (*B*) neurons. In control cells Thy-1 is present specifically in the axons (indicated by arrowheads) and does not colocalize with the dendritic marker. In FB1-treated neurons the axonal-exclusive Thy-1 labeling (in green; axons are indicated by arrowheads) is lost and dendrites appear yellow because of the colocalization of MAP2 and Thy-1. The dendritic distribution of the glutamate receptor 1 in control cells (not shown) does not change after FB1 treatment, and the protein (*D*) colocalizes with the dendritic marker MAP2 (*C*) whereas the axon of the cell (arrowheads) remains unstained.

neurons only 19, 26, and 13% of the newly synthesized mature HA was insoluble after 0, 25, and 60 min of chase, respectively. In untreated neurons the insolubility of HA increased with time after synthesis and 20, 50, and 45% of the protein was found in the pellet at the respective chase times.

Next we analyzed by immunofluorescence microscopy the solubility of the endogenous Thy-1 by inhibiting GSL and sphingomyelin synthesis with FB1 (33) (Fig. 4). After Triton X-100 extraction of control neurons Thy-1 was seen on axons (Fig. 4 *A* and *B*). Contrarily, Triton X-100 extraction in the FB1-treated neurons resulted in the total disappearance of Thy-1 (Fig. 4 *C* and *D*).

These results show that in polarized neurons both sphingolipids and cholesterol are responsible for the detergent insolubility of Thy-1 and HA.

Sphingolipid Depletion Affects the Sorting of Thy-1. The question then is, do protein–lipid rafts play a role in axonal sorting? To answer this we used the sphingolipid-synthesis inhibitor FB1 and determined the distribution of Thy-1. Digitalized images from 20 independent fields for both FB1-treated and control neurons were analyzed. In control neurons Thy-1 was found exclusively axonal in 60% of the cells (Fig. 5*A*); in 30%, the protein could not be detected, and in 10%, Thy-1 was found on both the axonal and dendritic surfaces. An identical result was obtained after treatment with 10 μM FB1. With 25 μM FB1 we observed exclusive axonal labeling in only 12% of the cells; in 45% of the cells Thy-1 was found missorted to both axonal and dendritic surfaces (Fig. 5*B*), and in the remaining cells Thy-1 immunoreactivity was not detected. Using this concentration of drug, cell viability was not affected and the neurite growth was equivalent to controls (not shown). Finally, the treatment with 40 μM FB1 also caused Thy-1 missorting, but in this case cell viability was seriously affected.

To test whether sphingolipid depletion with FB1 specifically altered axonal but not dendritic sorting we determined the distribution of a dendritic membrane protein, the glutamate receptor subunit GluR1, after the treatment. In FB1-treated neurons the exclusive dendritic distribution of GluR1, as well as that of the cytoskeletal protein MAP2, was not affected (Fig. 5 *C* and *D*).

Altogether the results directly demonstrate the specific involvement of sphingolipids in axonal sorting.

DISCUSSION

In this work we have used cultured hippocampal neurons to analyze the existence of DIGs and their possible role in axonal sorting. We observed that two membrane proteins, HA and Thy-1, are axonal and are included in DIGs in fully mature hippocampal neurons. We also observed that the ability to partition into DIGs is directly correlated with normal levels of cholesterol, GSL, and sphingomyelin and, more importantly, that when the formation of DIGs is disturbed by inhibition of lipid synthesis the normal sorting of Thy-1 is altered. These data strongly suggest that sphingolipid–cholesterol rafts play an important role in the axonal sorting of HA and Thy-1.

The Role of DIGs in Axonal Sorting. The possible role of DIGs in membrane sorting arises from studies in epithelial cells and is largely based on the demonstration that a set of apical proteins partition into detergent-insoluble complexes rich in sphingomyelin, GSL, and cholesterol and that the apical delivery of these proteins is impaired by disturbing the metabolism of the lipids (8). Our work shows the involvement of DIGs in axonal sorting by both biochemical and functional assays. By biochemistry we demonstrate that HA and Thy-1 behave like DIGs proteins; their resistance to detergent extraction is due to their binding to lipids. We also show that two dendritic proteins, an overexpressed viral glycoprotein, SFV E2, and a glutamate receptor subunit do not partition into DIGs. This result is important in several aspects. First, it shows that fully polarized neurons use the formation of lipid–protein complexes as a mechanism for the axonal delivery of mem-

brane proteins. Second, it confirms the hypothesis that the sorting mechanism, at least regarding these two proteins, is highly conserved in epithelial and neuronal cells. That reduction of the levels of cholesterol and sphingolipids led to a significant solubilization of both HA and Thy-1 shows the importance of these lipids in DIG formation. Moreover, inhibition of ceramide synthesis, the precursor of sphingolipids, with FB1 caused randomization of the distribution of Thy-1 to axons and dendrites. These findings are identical to the effects of cholesterol depletion in the transport and sorting of HA in MDCK cells (32) and to the effects of sphingolipid synthesis inhibition in the sorting of GPI-anchored proteins in the same cells (34). In contrast to the involvement of sphingolipids in neuronal membrane sorting is the report that FB1 does not affect the polarized distribution of synaptophysin and Thy-1 in cultured hippocampal neurons (35). The most obvious explanation for this discrepancy is that we observed an effect on sorting only at 25 μM of FB1, more than twice the concentration used in Schwarz *et al.* (35). Indeed, 10 μM FB1 did not impair sorting in our experiments. It is also important to note that the axonal protein synaptophysin is not included in DIGs and remains in the heaviest fractions after sucrose gradient centrifugation (not shown).

DIGs as a Discriminating Mechanism. Although our results with the axonal HA and Thy-1 suggest that DIG formation is a mechanism involved in axonal sorting, present evidence suggests that more than one vesicular route, and therefore more than one sorting mechanism, exists from the TGN to the axonal surface (36). Therefore, we assume that a sphingolipid–cholesterol raft mechanism will only account for the delivery of a subset of axonal proteins. One possibility is that neurons need to precisely target different proteins to the different functional domains of the axonal membrane; i.e., the axonal hillock, the nodes of Ranvier, the presynaptic terminals, the axonal shaft, or the active zone. Hence, DIG formation could serve as one of the mechanisms that guarantees precise sorting to one of these membrane subcompartments. This could be similar to what happens in epithelial cells in which not all the apically targeted proteins are raft-associated (34, 37, 38) or in oligodendrocytes in which DIGs appear to be required for the targeting of GPI-anchored proteins to the myelin sheath (39).

Our results reveal a mechanism for axonal sorting of a subset of axolemmal proteins and confirm that neuronal and epithelial cells use the same molecular machinery to distribute HA and Thy-1 to the axonal and apical surface, respectively. That we used a primary culture system, which morphologically and functionally resembles neurons *in situ*, suggests that in the brain, neurons may also utilize such sorting mechanisms to form and maintain a functional axonal membrane. The involvement of GSL–cholesterol rafts in both myelin formation (39) and axonal sorting (this work) may explain why patients with certain types of Niemann–Pick disease, in which cholesterol or sphingomyelin metabolism is altered, show dramatic neurological defects (40).

We thank H. Virta for providing virus stocks and HA antibody, Dr. Sanchez for polyclonal anti-MAP2, Renate Luedecke from MSD Sharp & Dohme for the gift of lovastatin, L. Meyn, A. Fradagrada, and B. Hellias for technical assistance, and P. Keller and P. Scheiffele for discussions and advice. M.D.L. is supported by an European Economic Community fellowship, and C.G.D. is supported by a Sonderforschungbereich (SFB 317) grant.

1. Dotti, C. G. & Simons, K. (1990) *Cell* **62,** 63–72.
2. Dotti, C. G., Kartenbeck, J. & Simons, K. (1993) *Brain Res.* **610,** 141–147.
3. Dotti, C. G., Parton. R. G. & Simons K. (1991) *Nature (London)* **349,** 158–161.
4. Pietrini, G., Suh, Y. J., Edelmann, L., Rudnick, G. & Caplan, M. J. (1994) *J. Biol. Chem.* **269,** 4668–4674.
5. de Hoop, M., von Poser, C., Lange, C., Ikonen, E., Hunziker, W. & Dotti, C. G. (1995) *J. Cell Biol.* **130,** 1447–1459.
6. Matter, K & Mellman, I. (1994) *Curr. Opin. Cell. Biol.* **6,** 545–554.
7. Simons, K., Dupree, P., Fiedler, K., Huber, L., Kobayashi, T., Kurzchalia, T., Olkkonen, S., Pimplikar, S., Parton, R. & Dotti, C. (1992) *Cold Spring Harbor Symp. Quant. Biol.* **LVII,** 611–619.
8. Simons, K. & Ikonen, E. (1997) *Nature (London)* **387,** 569–572.
9. van Meer, G., Stelzer, E. H. K., Wijnaendts-van-Resandt, R. W. & Simons, K. (1987) *J. Cell. Biol.* **105,** 1623–1635.
10. Simons, K. & van Meer, G. (1988) *Biochemistry* **27,** 6197–6202.
11. Simons, K. & Wandinger-Ness, A. (1990) *Cell* **62,** 207–210.
12. Skibbens, J. E., Roth, M. G. & Matlin, K. S. (1989) *J. Cell. Biol.* **108,** 821–832.
13. Brown, D. A. & Rose, J. K. (1992) *Cell* **68,** 533–544.
14. Fiedler, K., Kobayashi T., Kurzchalia, T. V. & Simons, K. (1993) *Biochemistry* **32,** 6365–6373.
15. Melkonian, K. A., Chu, T., Tortorella, L. B. & Brown, D. A. (1995) *Biochemistry* **34,** 16161–16179.
16. Schroeder, R. E., London, E. & Brown, D. (1994) *Proc. Natl. Acad. Sci. USA* **91,** 12130–12134.
17. Hanada, K., Nishijima, M., Akamatsu, Y. & Pagano, R. E. (1995) *J. Biol. Chem.* **270,** 6254–6260.
18. Scheiffele, P., Roth, G. R. & Simons, K. (1997) *EMBO J.* **16,** 5501–5508.
19. Goslin, K. & Banker, G. (1991) in *Culturing Nerve Cells*, eds. Banker, G. & Goslin, K. (MIT Press, Cambridge, MA), pp. 251–282.
20. Matlin, K. S., Reggio, H., Helenius, A. & Simons, K. (1981) *J. Cell. Biol.* **91,** 601–613.
21. Fuller, S., von Bonsdorf, K. H. & Simons, K. (1985) *EMBO J.* **4,** 2475–2485.
22. Cid-Arregui, A., Parton, R. G., Simons, K. & Dotti, C. G. (1995) *J. Neurosci.* **15,** 4259–4269.
23. Lisanti, M. P., Sargiacomo, M., Graeve, L., Saltiel, A. R. & Rodriguez-Boulan, E. (1988) *Proc. Natl. Acad. Sci. USA* **85,** 9557–9561.
24. Burke, B., Walter, C., Griffiths, G. & Warren, G. (1983) *Eur. J. Cell. Biol.* **31,** 315–324.
25. Caceres A., Banker, G., Steward, O., Binder, L. & Payne, M. (1984) *Dev. Brain. Res.* **13,** 314–318.
26. Craig, A. M., Blackstone, C. D., Huganir, R. L. & Banker, G. (1994) *Neuron* **10,** 1055–1068.
27. Alberts, A. W., Chen, J., Kuron, G., Hunt, V., Huff, F., Hoffman, C., Rothrock, J., Lopez, M., Joshua, H., Harris, E., *et al.* (1980) *Proc. Natl. Acad. Sci. USA* **77,** 3957–3961.
28. Kilsdonk, E. P. C., Yancey, P. G., Stoudt, G. W., Bangerter, F. W., Johnson, W. J., Phillips, M. C. & Rothblat, G. H. (1995) *J. Biol. Chem.* **270,** 17250–17256.
29. Neufeld, E. B., Cooney, A. M., Pitha, J., Dawidowicz, E. A., Dwyer, N. K., Pentchev, P. G. & Blanchette-Mackie, E. J. (1996) *J. Biol. Chem.* **271,** 21604–21613.
30. Ohtani, Y., Irie, K., Uekama, K., Fukunaga, K. & Pitha, J. (1989) *Eur. J. Biochem.* **186,** 17–22.
31. Brown, M. S. & Goldstein, J. L. (1980) *J. Lipid. Res.* **21,** 505–517.
32. Keller, P. & Simons, K. (1998) *J. Cell. Biol.,* in press.
33. Harel, R. & Futerman, A. H. (1993) *J. Biol. Chem.* **268,** 14476–14481.
34. Mays, R. W., Siemers, K. A., Fritz, B. A., Lowe, A. W., van Meer, G. & Nelson, W. J. (1995) *J. Cell. Biol.* **130,** 1105–1115.
35. Schwarz, A., Rapaport, E., Hirschberg, K. & Futerman, A. H. (1995) *J. Biol. Chem.* **270,** 10990–10998.
36. Okada, Y., Yamazaki, H., Sekine-Aizawa, Y. & Hirokawa, N. (1995) *Cell* **81,** 769–780.
37. Mostov, K. E., Apodaca, G., Aroeti, B. & Okamoto, C. (1992) *J. Cell. Biol.* **116,** 577–583.
38. Nicolas, F., Tiveron, M. C., Davoust, J. & Reggio, H. (1994) *J. Cell. Sci.* **107,** 2679–2698.
39. Kramer, E. M., Koch, T., Niehaus, A. & Trotter, J. (1997) *J. Biol. Chem.* **272,** 8937–8945.
40. Brady, R. (1987) in *The Metabolic Basis of Inherited Disease*, eds. Stanbury, J. B., Wyngaarden, J. B., Friedrichson, D. S., Goldstein, J. L. & Brown, M. S., eds. (McGraw–Hill, New York), pp. 831–841.